

Recent progress on the vortex filament equation for regular polygons

✉ Sandeep Kumar

BCAM - Basque Center for Applied
Mathematics
skumar@bcamath.org

Abstract: Due to its simplicity and geometric structure, the vortex filament equation (VFE) secures a unique place in fluid literature. The equation is a model for the dynamics of a vortex filament (e.g., smoke rings, tornadoes, etc.) in a three-dimensional inviscid incompressible fluid. In this work, we describe recent progress on its behaviour for the polygonal-shaped filaments curves. More precisely, we concentrate on the evolution of VFE for regular polygons as the initial data. Besides problem formulation, addressing it using theoretical and numerical techniques, we discuss the time evolution of a single point located on the curve which, in turn, follows a multifractal trajectory. Simultaneously, we also consider the corresponding problem in the hyperbolic 3-space.

Resumen: Debido a su simplicidad y estructura geométrica, la *vortex filament equation* (VFE) ocupa un lugar único en la literatura de fluidos. La ecuación modela la dinámica de un filamento de vórtice (p. ej., anillos de humo, tornados, etc.) en un fluido incompresible no viscoso tridimensional. En este trabajo, describimos los avances recientes en su comportamiento para las curvas de filamentos de forma poligonal. Más precisamente, nos concentramos en la evolución de la VFE para polígonos regulares como datos iniciales. Además de la formulación del problema, abordando el mismo mediante técnicas teóricas y numéricas, se comenta la evolución temporal de un único punto ubicado en la curva que, a su vez, sigue una trayectoria multifractal. Simultáneamente, también consideramos el problema correspondiente en el 3-espacio hiperbólico.

Keywords: vortex filament equation, Schrödinger map equation, numerical methods for PDEs, multifractality, Talbot effect.

MSC2010: 35Q55, 35Q56, 35Q35.

Acknowledgements: This work has been supported by the ERCEA Advanced Grant 2014 669689 - HADE, Severo Ochoa grant SEV-2017-0718, and the Basque Government BERC Program 2018-2021.

Reference: KUMAR, Sandeep. "Recent progress on the vortex filament equation for regular polygons". In: *TEMat monográficos*, 2 (2021): *Proceedings of the 3rd BYMAT Conference*, pp. 235-238. ISSN: 2660-6003. URL: <https://temat.es/monograficos/article/view/vol2-p235>.

1. Introduction

The vortex filament equation (VFE) is a simplified model that describes the dynamics of an ideal fluid whose vorticity is concentrated on a curve called vortex filament, i.e., smoke rings, tornadoes, etc. Given by Da Rios in his PhD thesis in 1906, for an arc-length parametrized curve \mathbf{X} representing a vortex filament in three-dimensions, the VFE is expressed as [8]

$$(1) \quad \mathbf{X}_t = \mathbf{X}_s \wedge \mathbf{X}_{ss}, \quad s \in \mathbb{R}, t \in \mathbb{R},$$

where \wedge is the usual cross-product, s arc-length and t time parameter, and subscripts denote the partial derivatives. The tangent vector $\mathbf{T} = \mathbf{X}_s$ solves the so-called Schrödinger map equation onto the sphere

$$(2) \quad \mathbf{T}_t = \mathbf{T} \wedge \mathbf{T}_{ss}.$$

Due to its geometrical structure and properties, in the simplest form, (2) allows \mathbf{T} to take its value on the Euclidean unit sphere $\mathbb{S}^2 = \{(x_1, x_2, x_3) : x_1^2 + x_2^2 + x_3^2 = 1\}$, or, a hyperbolic one, i.e., $\mathbb{H}^2 = \{(x_1, x_2, x_3) : -x_1^2 + x_2^2 + x_3^2 = -1, x_1 > 0\}$. Note that, when $\mathbf{T} \in \mathbb{H}^2$, \mathbf{X} lies in the Minkowski 3-space $\mathbb{R}^{1,2} = \{(x_1, x_2, x_3) : ds^2 = -dx_1^2 + dx_2^2 + dx_3^2\}$, and the cross product in (1)–(2) is given by $\mathbf{a} \wedge \mathbf{b} = (-a_2b_3 - a_3b_2, a_3b_1 - a_1b_3, a_1b_2 - a_2b_1)$. Moreover, with the curvature κ , torsion τ , the tangent \mathbf{T} , normal \mathbf{n} and binormal \mathbf{b} vectors of \mathbf{X} form an orthonormal system and solve the Frenet–Serret formulas

$$(3) \quad \begin{pmatrix} \mathbf{T} \\ \mathbf{n} \\ \mathbf{b} \end{pmatrix}_s = \begin{pmatrix} 0 & \kappa & 0 \\ \mp\kappa & 0 & \tau \\ 0 & -\tau & 0 \end{pmatrix} \cdot \begin{pmatrix} \mathbf{T} \\ \mathbf{n} \\ \mathbf{b} \end{pmatrix},$$

where the minus sign refers to the Euclidean and the plus sign to the hyperbolic cases. With this, in 1972, Hasimoto developed a relationship between (1)–(2) and the cubic nonlinear Schrödinger (NLS) equation where the unknown is the wave function $\psi(s, t) = \kappa(s, t)e^{i \int_0^s \tau(s', t) ds'}$. Thanks to this connection, any advancement in the direction of (1)–(2) is equivalent to that for the NLS equation as well.

Apart from the explicit solutions of VFE, i.e., circle, straight line and helix, another important class is the one-parameter family of the self-similar solutions which are characterized by a parameter $c_0 > 0$. In both Euclidean and hyperbolic cases, for a given time $t > 0$, the curve \mathbf{X} has a curvature c_0/\sqrt{t} and a torsion $s/2t$ and it has been shown that, as the time t tends to zero, it develops a corner and turns into two non-parallel straight lines meeting at $s = 0$. This implies that, at $t = 0$, the corresponding tangent vector is a Heaviside-type function and the initial solution of the NLS equation is a Dirac delta located at $s = 0$. The so-called *one-corner problem* has been well studied by Gutierrez et. al. and Banica et. al. theoretically, and by Buttke and de la Hoz numerically in their PhD theses.

2. Some polygonal solutions of (1)–(2)

Motivating from curves with one corner otherwise smooth, it is natural to address the evolution of (1)–(2) for curves with several corners. In this direction, we consider the simplest case of regular planar polygons in both Euclidean and hyperbolic spaces followed by their extension to respective non-planar ones.

2.1. Regular planar polygons

The evolution of (1)–(2) for $\mathbf{X}(s, 0)$ as a regular planar polygon is equivalent to that of the NLS equation with initial datum $\psi(s, 0) = c_0 \sum_{k \in \mathbb{Z}} \delta(s - k\Delta s)$, where Δs is the side-length of the initial polygonal curve which is equal to $2\pi/M$ for an M -sided polygon in the Euclidean space and $l > 0$ for a hyperbolic polygon and c_0 depends on the initial configuration of the curve [3, 5]. By assuming uniqueness and using the Galilean invariance of the NLS equation, followed by algebraic calculations, the time evolution of \mathbf{X} and \mathbf{T} can be described up to a rigid movement for the rational multiples of the time-period. The numerical experiments confirm that depending on the (denominator of) rationals, the polygonal curve develops more number of sides, a behaviour reminiscent of the Talbot effect in optics. For the numerical computations, due to the

2π spatial periodicity of \mathbf{T} , a pseudo-spectral discretization is used in the Euclidean case; however, for the hyperbolic case, a finite difference scheme with Dirichlet boundary conditions on \mathbf{T} is employed; a fourth-order Runge–Kutta method is used for the time evolution in both cases.

Furthermore, the time evolution of a single point, i.e., $\mathbf{X}(0, t)$ lies in a plane. This is displayed in Figure 1, for an equilateral triangle which also shows that with a vertical translation at half time-period $t = \pi/M^2$, the triangle appears upside down and reappears at the end of the time-period $t = 2\pi/M^2$. The latter is recorded as the axis-switching phenomenon in fluid literature, for example, non-circular jets (for a qualitative comparison see evolutions of an [equilateral triangle](#), and a [vortex filament](#)). The right-hand side of each subfigure in Figure 1 shows the projection of $\mathbf{X}(0, t)$ onto \mathbb{C} and the same after removing the vertical height, denoted by $z_M(t)$ (or, $z_l(t)$ in the hyperbolic case). Nonetheless, as M becomes larger (or l smaller), $z_M(t)$ (or $z_l(t)$), converges to the so-called Riemann's non-differentiable, given by the real part of $\phi(t) = \sum_{k=1}^{\infty} \frac{e^{i\pi k^2 t}}{i\pi k^2}$, $t \in [0, 2]$, see Figure 2. Due to its multifractal character, the function ϕ is an important object whose properties were studied by Jaffard in [6], and recently by Eceizabarrena in [2].

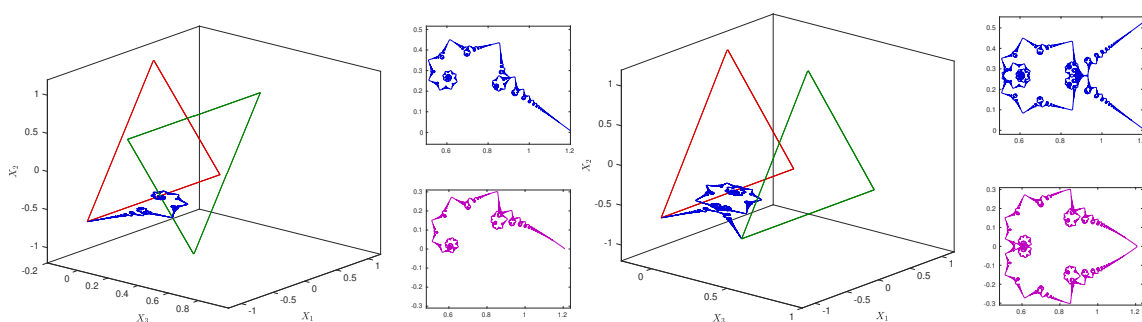


Figure 1: For $M = 3$, $\mathbf{X}(s, 0)$ (red), $\mathbf{X}(s, t)$ (green), $\mathbf{X}(0, t_0)$, $t_0 \in [0, t]$ (blue) at $t = \frac{\pi}{M^2}$ (left), $\frac{2\pi}{M^2}$ (right).

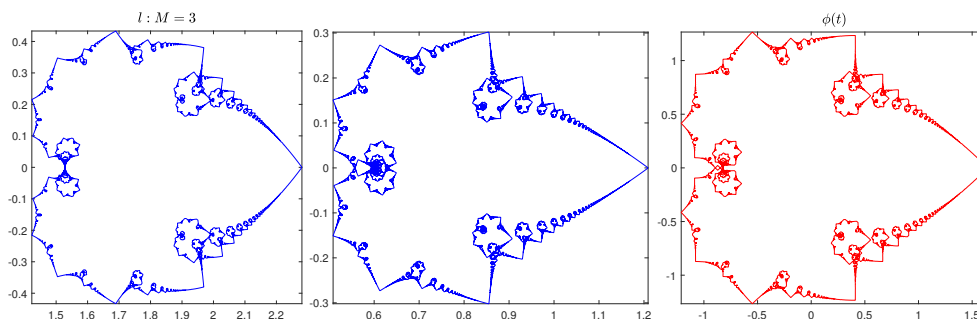


Figure 2: $z_l(t)$, $z_M(t)$, for $M = 3$ (see [3, 5] for their precise definition), and $\phi(t)$.

2.2. Regular polygons with a nonzero torsion

For the arc-length parameterized \mathbf{X} , the nonzero torsion can be introduced with the parameter b . In the Euclidean case, $b \in [-1, 1]$ corresponds to the third component of the tangent vector, whereas $b \in (-\infty, -1] \cup [1, \infty)$ as the first component of $\mathbf{T} \in \mathbb{H}^2$, and $b \in (-\infty, \infty)$ as the third component result in the *circular helix* and *hyperbolic helix*, respectively [4, 7]. Note that $b = 0$ reduces back to the planar case discussed above. In both settings, together with the parameters M or l (giving side-length), b determines the curvature angle ρ_0 and torsion angle θ_0 . Moreover, by denoting ψ as ψ_θ when $\theta_0 > 0$, we have

$$(4) \quad \psi_\theta(s, 0) = c_{\theta,0} e^{i\gamma s} \sum_{k \in \mathbb{Z}} \delta(s - k\Delta s) = \frac{c_{\theta,0}}{c_0} e^{i\gamma s} \psi(s, 0),$$

with $\gamma = \theta_0/\Delta s$, and $c_{\theta,0} > 0$, Δs , suitably chosen as mentioned above. Besides the algebraic solution, with the numerical simulations, we detect the aperiodic movement of a corner initially at $s = 0$ (e.g., see

the [link](#)) and categorize it as *Galilean shift* and *phase shift* which also implies that $\mathbf{X}(0, t)$ is non-planar. With a Fourier analysis of $\mathbf{X}(0, t)$ at a numerical level, different variants of $\phi(t)$ have been found whose structure, in turn, depends on the initial torsion. More precisely, for $\theta_0 = \pi c/d$, $c, d \in \mathbb{N}$, $\gcd(c, d) = 1$, the vertical movement of $\mathbf{X}(0, t)$ can be compared with the imaginary part of $\phi_{c,d}(t) = \sum_{k \in A_{c,d}} \frac{e^{2\pi i k t}}{k}$, to which it converges as M tends to infinity or l to zero (i.e., $\mathbf{X}(s, 0)$ to a smooth helix), with

$$(5) \quad t \in \begin{cases} [0, 1/2] & \text{if } c \cdot d \text{ odd,} \\ [0, 1] & \text{if } c \cdot d \text{ even,} \end{cases} \quad A_{c,d} = \begin{cases} \{n(nd + c)/2 \mid n \in \mathbb{Z}\} \cap \mathbb{N} & \text{if } c \cdot d \text{ odd,} \\ \{n(nd + c) \mid n \in \mathbb{Z}\} \cap \mathbb{N} & \text{if } c \cdot d \text{ even.} \end{cases}$$

Similarly, strong numerical evidence is given that, for a given M and as b approaches 1 (i.e., $\mathbf{X}(s, 0)$ to a straight line), the stereographic projection of $\mathbf{X}(0, t)$ onto \mathbb{C} tends to $\phi_M(t) = \sum_{k \in A_M} \frac{e^{2\pi i k^2 t}}{k^2}$, $t \in [0, 1]$, where $A_M = \{1\} \cup \{nM \pm 1 \mid n \in \mathbb{N}\}$. Remark that, for $\theta_0 \neq 0$, $\psi_\theta(s, 0)$ is quasi-periodic and becomes 2π -periodic when $b \rightarrow 1$. Thus, through a very formal computation if, instead of the NLS equation, one solves the initial value problem for the free Schrödinger equation $\psi_t = i\psi_{ss}$, for (4) with $b \approx 1$, then

$$\hat{\psi}_\theta(k, t) = e^{-ik^2 t} \hat{\psi}_\theta(k, 0), \text{ with } \hat{\psi}_\theta(k, 0) = \begin{cases} \frac{M}{2\pi} & \text{if } k \pm 1 = nM, n \in \mathbb{N}, \\ 0 & \text{else.} \end{cases}$$

Then, bearing in mind the Hasimoto transformation and (1)–(3), $\mathbf{X}(0, t)$ can be related to $\int_0^t \psi_\theta(s, \tilde{t}) d\tilde{t}$, with $s = 0$, which computed using $\hat{\psi}_\theta(k, t)$ is ϕ_M up to a scaling factor. Nonetheless, the existence of ϕ and its variants in the evolution of $\mathbf{X}(0, t)$ has been proved rigorously by Banica and Vega recently in [1].

3. Conclusion

Thus, the appearance of Riemann's function (and its variants) in the evolution of polygonal curves indicates that the evolution of (1)–(2) for smooth curves is not stable. That is, as the number of sides M tends to infinity (or l to zero), the polygonal curve approaches a smooth curve; however, when measured in the right topology, the trajectory of a single particle located on it converges to a multifractal, unlike that of a smooth curve (to compare, see the [link](#)). Recall that Riemann's function satisfies the multifractal formalism proposed by Frisch and Parisi [6]. Therefore, these latest results also contribute to the debate, which is already more than a one-hundred-year-old, on the validity of the vortex filament equation as a simplified model for understanding fundamental but complex natural phenomena such as turbulence.

References

- [1] BANICA, Valeria and VEGA, Luis. “Riemann's non-differentiable function and the binormal curvature flow”. In: *arXiv e-prints* (2020). arXiv: 2007.07184 [math.AP].
- [2] ECEIZABARRENA, Daniel. “Geometric differentiability of Riemann's non-differentiable function”. In: *Advances in Mathematics* 366 (2020), n.º 107091.
- [3] DE LA HOZ, Francisco; KUMAR, Sandeep, and VEGA, Luis. “Vortex Filament Equation for a regular polygon in the hyperbolic plane”. In: *arXiv e-prints* (2020). arXiv: 2007.04944 [math.NA].
- [4] DE LA HOZ, Francisco; KUMAR, Sandeep, and VEGA, Luis. “On the Evolution of the Vortex Filament Equation for regular M -polygons with nonzero torsion”. In: *SIAM Journal on Applied Mathematics* 80.2 (2020), pp. 1034–1056.
- [5] DE LA HOZ, Francisco and VEGA, Luis. “Vortex filament equation for a regular polygon”. In: *Nonlinearity* 27.12 (2014), pp. 3031–3057.
- [6] JAFFARD, Stéphane. “The spectrum of singularities of Riemann's function”. In: *Revista Matemática Iberoamericana* 12.2 (1996), pp. 441–460.
- [7] KUMAR, Sandeep. “On the Schrödinger map for regular helical polygons in the hyperbolic space”. In: *arXiv e-prints* (2020). arXiv: 2010.12045 [math.AP].
- [8] DA RIOS, Luigi Sante. “Sul moto d'un liquido indefinito con un filetto vorticoso di forma qualunque”. In: *Rendiconti del Circolo Matematico di Palermo (1884-1940)* 22.1 (1906), pp. 117–135.